Heliyon 10 (2024) e27194

Contents lists available at ScienceDirect

Heliyon

journal homepage: www.cell.com/heliyon

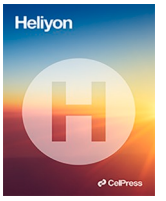

Research article

Discovering ferroptosis-associated tumor antigens and ferroptosis subtypes in pancreatic adenocarcinoma to facilitate mRNA vaccine development

Ting Yan [a], Lingxiang Wang [b,*]

[a] Department of General Surgery, Second Affiliated People's Hospital, Fujian University of Traditional Chinese Medicine, Fuzhou, Fujian, China
[b] Department of General Surgery, Second Xiangya Hospital, Central South University, Changsha, Hunan, China

ARTICLE INFO

Keywords:
Pancreatic cancer
mRNA vaccine
Ferroptosis subtypes
Tumor immunity
Ferroptosis landscape

ABSTRACT

Pancreatic adenocarcinoma (PAAD) is an aggressive, heterogeneous malignancy. We studied the potential of ferroptosis-related tumor vaccines for PAAD treatment. Ferroptosis-related genes, gene expression profiles, and clinical information were extracted from the FerrDB, UCSC Xena, and International Cancer Genome Consortium databases. Differential expression levels and prognostic indices were calculated, genetic alterations and correlations with immune-infiltrating cells were explored, and consensus clustering analysis was performed to identify ferroptosis subtypes and gene modules. Immune enrichment scores were calculated using gene set enrichment analysis, and gene modules were screened using weighted gene co-expression network analysis. The ferroptosis subtype distribution was visualized using graph learning-based dimensionality reduction analysis of the Monocle package with a Gaussian distribution. We identified four ferroptosis-related tumor antigens, AGPS, KDM5A, NRAS, and OSBPL9, which were associated with pancreatic cancer prognosis and antigen-presenting cell infiltration. We determined three minor ferroptosis subtypes, with different clinical prognosis and tumor immune status. Of the subtypes, FS3 may be more suitable for mRNA therapy. We constructed a PAAD ferroptosis landscape to identify the ferroptosis status of patients and predict their prognosis. Finally, we found that the eigengene of the green module was an independent prognostic factor, with a significantly better prognosis in the high-score group than in the low-score group. In conclusion, we identified four ferroptosis-related genes as targets for mRNA vaccines and three ferroptosis subtypes, providing a theoretical basis for the anti-PAAD mRNA vaccine and defining suitable patients for vaccination.

1. Introduction

Pancreatic cancer is an extremely malignant and aggressive tumor, with a 5-year survival rate of 11%, significantly lower than other cancers such as prostate cancer (98%), melanoma (93%), and female breast cancer (90%). The most prevalent type of pancreatic cancer is pancreatic adenocarcinoma (PAAD), which accounts for approximately 90% of all cases [1]. Pancreatic cancer cases continue to increase, and it is predicted that by 2030, pancreatic cancer will be one of the deadliest cancers [2,3]. Due to the deep anatomical location of the pancreas, the signs and symptoms of pancreatic cancer do not appear until it has advanced to a later stage, resulting in

* Corresponding author.
E-mail addresses: wang814515445@foxmail.com (T. Yan), wanglingxiang@csu.edu.cn (L. Wang).

https://doi.org/10.1016/j.heliyon.2024.e27194
Received 15 November 2023; Received in revised form 25 February 2024; Accepted 26 February 2024
Available online 3 March 2024

Abbreviations

APCs:	Antigen-Presenting Cells
DCs:	Dendritic Cells
DAMPs:	Damage-Associated Molecular Patterns
FRGs:	Ferroptosis-Related Genes
ICD:	Immunogenic Cell Death
ICP:	Immune Checkpoint
MSI:	Microsatellite instability
OS:	Overall Survival
PAAD:	Pancreatic adenocarcinoma
PFS:	Progression-free survival
ssGSEA:	Single-sample Gene Set Enrichment Analysis
TIMER:	Tumor Immune Estimation Resource
TNM:	Tumor,Node,Metastasis
TMB:	Tumor mutation burden
TME:	Tumor Microenvironment
WGCNA:	Weighted Gene Co-expression Network Analysis

less than 20% of patients being eligible for surgical resection at the time of diagnosis [4]. Beyond surgery, pancreatic cancer treatment options are extremely limited, and the progress of new treatments is very slow. Gemcitabine, a chemotherapy drug that has been used for over 20 years, remains the first-line treatment for patients with advanced pancreatic cancer, despite only a marginal improvement in overall survival (OS) [5]. Therefore, developing new strategies for treating pancreatic cancer is crucial for improving therapeutic outcomes.

In recent years, tumor immunotherapy has generated much excitement and achieved significant therapeutic effects. In particular, the combination of anti-CTLA4 and anti-PD-L1 checkpoint inhibition has emerged as a transformative breakthrough in the treatment of metastatic melanoma, increasing the 5-year relative survival rate for distant-stage disease from 15% to 30% [6]. Further research has focused on tumor vaccines as a strategy for cancer immunotherapy. Tumor vaccines refer to the use of tumor antigens to induce specific anti-tumor effects in the body through active immunity, which amplifies and maintains specific T cell responses to stimulate its own immune protection mechanisms, ultimately treating tumors or preventing recurrence [7]. Tumor antigens can be classified into peptide, tumor cell, dendritic cell, DNA, and RNA types [8]. Since mRNA is a non-infectious, non-integrating platform, there is no potential risk of infection or insertional mutagenesis compared to DNA vaccines and viral vector vaccines. Additionally, unlike traditional peptide vaccines, RNA sequences can be easily modified to encode any protein and stimulate the immune response itself [7]. These properties make mRNA vaccines a promising option for tumor immunotherapy.

Pancreatic cancer is known for its low immunogenicity and highly immunosuppressive tumor microenvironment (TME) [9]. The desmoplastic reaction to the tumor, which is a characteristic feature of the pancreatic ductal adenocarcinoma (PDAC) TME, leads to reduced angiogenesis, rendering the tissue insensitive to therapeutic drugs and causing poor infiltration of tumor immune cells [10]. To provide a favorable microenvironment for tumor growth, immune cells that could inhibit and kill tumor cells are downregulated, especially $CD8^+$ T cells, which play a critical role in recognizing and killing cancer cells as well as activating other immune cells to mount an effective immune response against cancerous tissue. This results in a state of immune tolerance, in which the immune system is unable to recognize or eliminate cancerous cells [11]. This allows tumor cells to continue growing, leading to disease progression and poor clinical outcomes.

Hence, the pursuit of novel strategies aimed at modifying the PAAD TME has emerged as a prominent research focus. Ferroptosis, an iron- and oxygen-dependent type of programmed cell death triggered by the accumulation of lipid peroxides [12], is emerging as an important mechanism for regulating cell death in cancer and other diseases. Recent research suggests that ferroptosis may play an important role in modulating the immune response to cancer. Ferroptosis-related lipoperoxides could serve as biomarkers of cell death and induce dendritic cells (DCs) to recognize, engulf, and process tumor cells. DCs could then present tumor-associated antigens to $CD8^+$ T lymphocytes, activating their cytotoxic effects and enhancing the therapeutic immunological effect against cancer [13]. In addition, ferroptotic cells release various damage-associated molecular patterns (DAMPs) and pro-inflammatory cytokines, interleukin-1β, and interleukin-18, which could further activate immune cells and enhance the immune response against tumors [14].

In this study, we identified four ferroptosis-related genes (FRGs) as targets for mRNA vaccines and validated three ferroptosis subtypes across different cohorts. The FS3 subtype showed greater response to vaccination. Clinical prognosis and tumor immune status differed among the subtypes. This could provide useful guidance for selecting suitable patients for vaccination.

2. Results

2.1. Identification of potential ferroptosis-related antigens in PAAD

To identify potential mRNA vaccines for PAAD, we conducted a screening for genes that exhibited atypical expression patterns. This

comprehensive analysis allowed us to identify a total of 9222 differentially expressed genes. Among these, 8741 genes were found to be overexpressed and may encode tumor-associated antigens when compared to normal tissue (Fig. 1A). We then screened 9135 mutated genes that might encode tumor-specific antigens by analyzing mutated gene segments and numbers in individual samples (Fig. 1B–C). Mutation analysis revealed that *KRAS* was the most commonly mutated gene in terms of mutation gene segments and counts (Fig. 1D–E). In addition, we observed significant mutations in *TP53, CDKN2A, CKDN2A-DT, SMAD4, CDKN2B-AS1,* and *MTAP*, regardless of mutation number or frequency. These gene mutations may play an important role in the occurrence and progression of PAAD. Combining the results of mutated and overexpressed genes, we identified 912 cancer-related genes that were frequently mutated and upregulated, which might serve as potential tumor antigens.

Subsequently, we focused on identifying mRNA antigens associated with FRGs. After conducting OS and PFS analyses, we identified 13 FRGs out of 912 potential antigens (Supplementary Fig. 1). Considering the interaction between tumor antigens and antigen-presenting cells (APCs), we further screened these potential antigens for their correlation with APCs using the TIMER database. *AGPS, KDM5A, NRAS,* and *OSBPL9* genes were found to be positively correlated with different APCs (Fig. 2A–D), and high expression had poorer OS and PFS (Supplementary Figs. 2A–H). Additionally, we found that the expression of these genes showed different trends in different TNM stages; however, all showed an increasing trend in late stage (Supplementary Figs. 3A–D). These findings indicate that the identified tumor antigens have the potential to be processed and presented by APCs to T cells, recognized by B cells, and trigger an immune response. Additionally, these genes might initiate ferroptosis in tumor cells, resulting in further eradication of cancer cells.

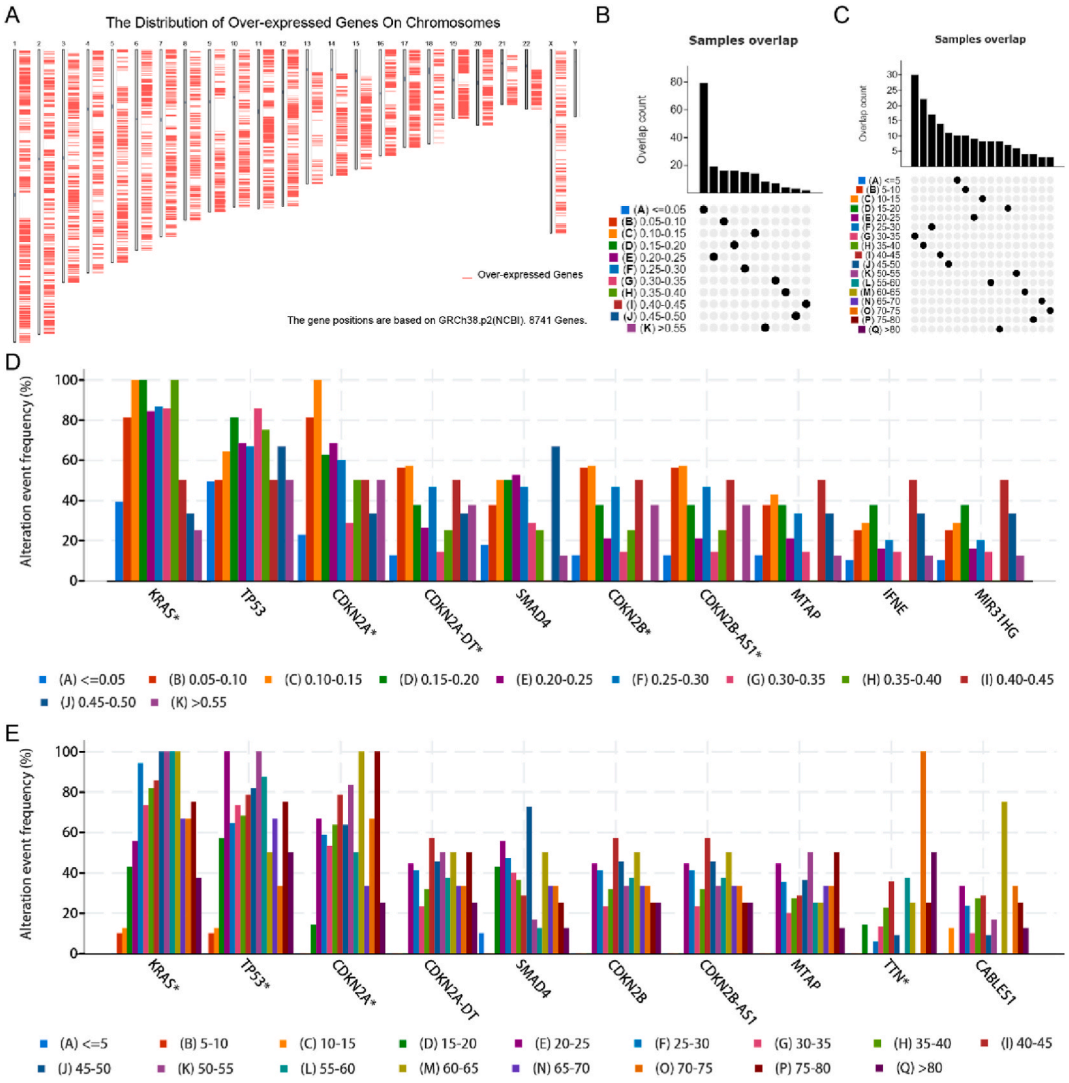

Fig. 1. Identification of potential tumor antigens in PAAD. (A): Identification of potential tumor-associated antigens in PAAD. Chromosome distribution of upregulated genes in PAAD. (B–E): Identification of potential tumor-specific antigens in PAAD. Samples overlap in (B) altered genomic segments and (C) mutation count array. The most frequently occurring genes in (D) altered genomic segments and (E) mutation count array. PAAD: Pancreatic adenocarcinoma.

2.2. Identification of potential ferroptosis subtypes in PAAD

Ferroptosis has been shown to play a significant role in killing tumor cells and is closely associated with tumor immunity. Identifying subtypes that reflect the status of ferroptosis in tumors and their microenvironment may help identify patients suitable for vaccination. Therefore, we analyzed the expression profiles of 424 FRGs in TCGA-PAAD for consensus clustering. Based on cumulative distribution functions and the area under the delta function, we selected k = 3 to stably cluster immune-related genes (Fig. 3A–B), obtaining three ferroptosis subtypes, identified as FS1, FS2, and FS3 (Fig. 3C). Consistent with the TCGA-PAAD cohort results, PACA-CA was also stratified into three ferroptosis subtypes (FS1, FS2, and FS3) (Fig. 3D). The PCA results showed a clear discrimination between the three ferroptosis subtypes (Fig. 3E). Prognostic analysis showed that FS3 was associated with a better prognosis in the TCGA-PAAD cohort, whereas FS1 and FS2 had lower survival probabilities (Fig. 3F). The three ferroptosis subtypes in PACA-CA showed the same significant prognostic differences; however, their differences were relatively small compared with the TCGA-PAAD cohort (Fig. 3G). The survival curves for FS3 exhibit notable discrepancies across the two datasets as depicted in Fig. 3F and G. The underlying reasons for this may include, firstly, the possibility that the datasets are derived from distinct populations, thereby

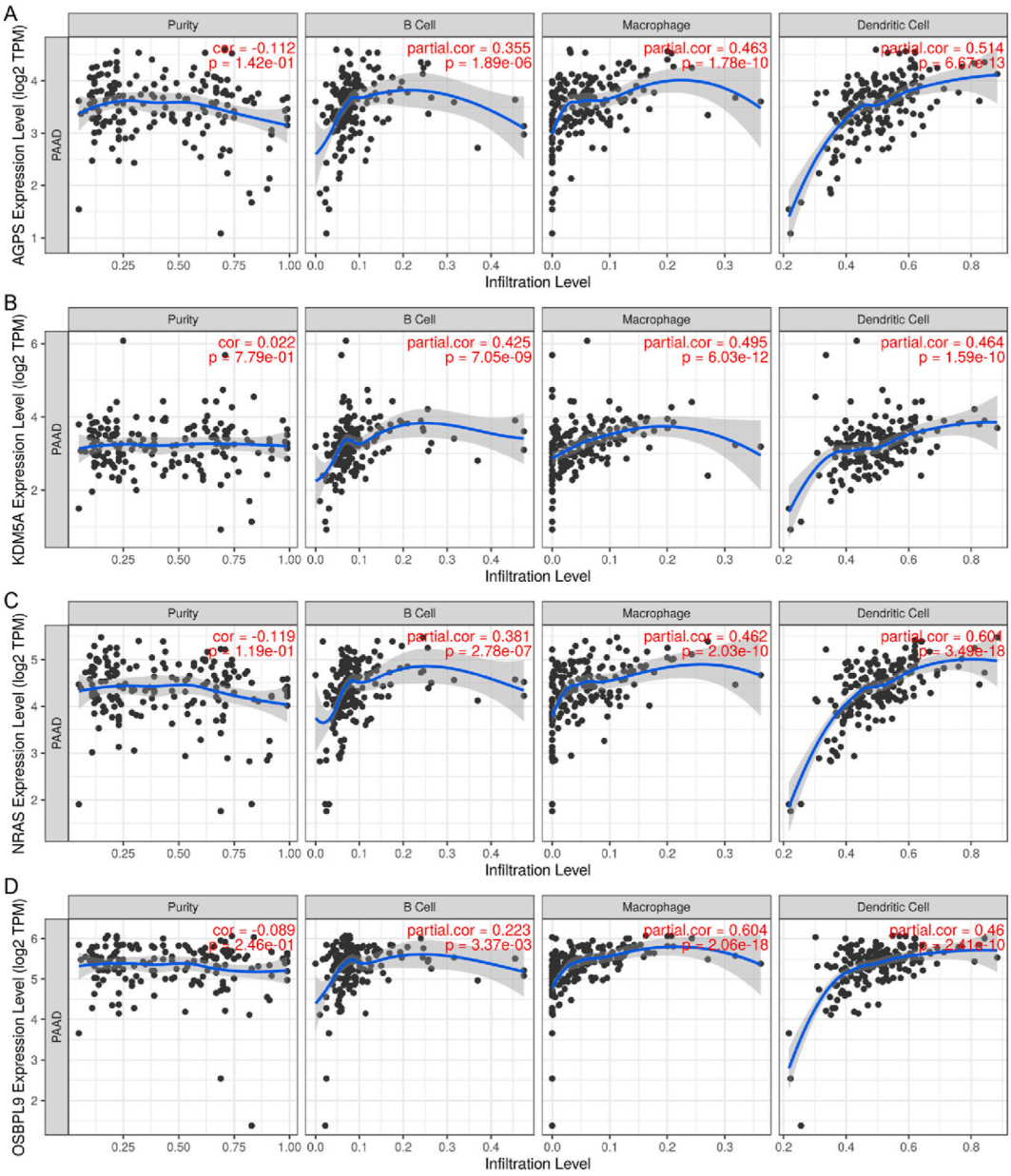

Fig. 2. Identification of tumor antigens related to APCs. Correlation between expression levels of *AGPS* (A), *KDM5A* (B), *NRAS* (C), and *OSBPL9* (D) in PAAD tumors and the purity of the tumor, as well as the infiltration of B cells, macrophages, and dendritic cells. APCs: Antigen-presenting cells.

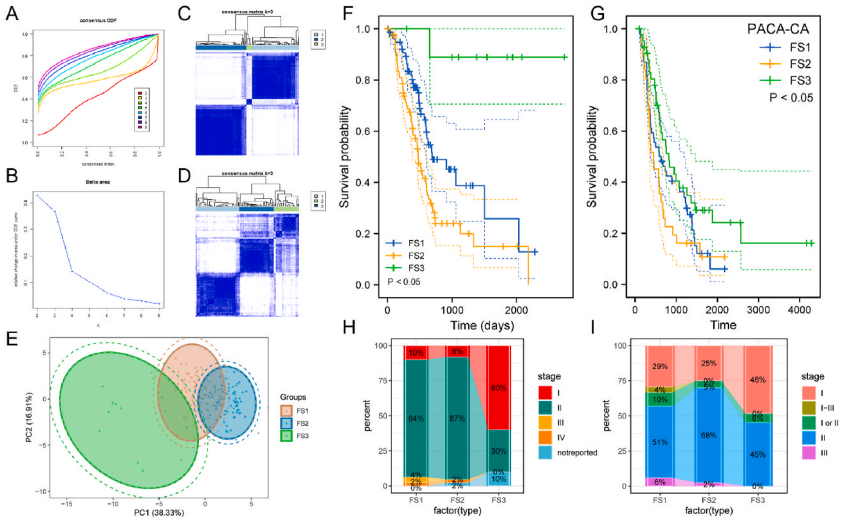

Fig. 3. Identification of potential ferroptosis subtypes in PAAD. (A) Cumulative distribution function curve of ferroptosis-related genes in the TCGA-PAAD cohort and (B) the area under the delta function. (C) Clustering heatmap of TCGA-PAAD samples and (D) PACA-CA samples. (E) Principal component analysis of ferroptosis subtypes in TCGA-PAAD. (F) Kaplan-Meier curves show overall survival of ferroptosis subtypes in the TCGA cohort and (G) PACA-CA cohort. (H) Distribution proportion of PAAD stages in different ferroptosis subtypes in TCGA-PAAD and (I) in PACA-CA.

introducing heterogeneity in sample composition that could potentially impact survival curves. Secondly, variations in environmental factors or treatment strategies may also play a role in influencing survival outcomes. Additionally, the relative trends among FS1, FS2, and FS3 are fundamentally consistent within both the PACA-CA and PAAD cohorts. This consistency indeed provides a measure of support for the validation of our model. In different stages, the three ferroptosis subtypes showed irregular distributions; early-stages had a higher proportion of the FS3 subtype, while mid-to late-stages had a higher proportion of the FS1 and FS2 subtypes (Fig. 3H–I). In summary, ferroptosis typing could be used to predict the prognosis of patients with PAAD and has been validated in different cohorts.

2.3. Relationship between ferroptosis subtypes and mutation status

Higher TMB and somatic mutation rates are associated with stronger anticancer immunity. Therefore, we calculated the TMB, MSI, and total number of mutations for each PAAD patient using the TCGA-PAAD mutation dataset and compared all ferroptosis subtypes. As shown in (Fig. 4A–B), The FS2 subtype exhibits the highest tumor mutational burden (TMB) and total number of mutations. There was no significant difference in MSI among the three ferroptosis subtypes; however, there was a trend of higher MSI in FS3 than in FS1 and FS2 (Fig. 4C). Additionally, 30 genes, including *TP53, KRAS,* and *CDKN2A,* showed different mutation states in different subtypes (Fig. 4D). These results suggest that TMB and mutation count could serve as potential indicators for the use of mRNA vaccines and that different ferroptosis subtypes have different mutational characteristics.

2.4. Relationship between ferroptosis subtypes and immune regulators in PAAD

Previous research has shown that ICPs, and ICD immune modulators, have a significant impact on the regulation of host antitumor immunity. This ultimately affects the efficacy of mRNA vaccines. Furthermore, a significant correlation between ferroptosis and immune regulation has been reported previously. Therefore, we evaluated the differential expression of ICP and ICD regulators among the three ferroptosis subtypes. In both cohorts, 25 ICD genes, including *ANXA1, HGF, and PANX1,* were detected with consistent expression trends in the different subtypes (Fig. 5A–B). Particularly, these genes were downregulated in the FS3 subtype compared to other subtypes. For ICP genes, 46 genes were detected in both cohorts, with different expression trends in the ferroptosis subtypes (Fig. 5C–D). Apart from elevated *CD200* expression, most ICP genes showed significantly lower expression in FS3 compared to FS1 and FS2. Additionally, a greater number of ICP genes exhibited differential expression among the three ferroptosis subtypes in the TCGA-PAAD cohort, which can be attributed to its larger sample size. In summary, ferroptosis subtypes could reflect the expression levels of ICD regulators and ICPs, and could serve as biomarkers for mRNA vaccines.

2.5. Cell and molecular characteristics of ferroptosis subtypes

Using the ESTIMATE algorithm, we found that there were more immune cell infiltrates in patients with FS1-type tumors, followed by FS2; FS3 had the least immune cell infiltrates (Supplementary Figs. 4A–B). Subsequently, we evaluated immune cell components in the three ferroptosis subtypes using ssGSEA to score 28 signature genes previously reported in the TCGA-PAAD and PACA-CA cohorts (Fig. 6A–B). Immune cell components were grouped into three clusters, and significant differences in the composition among the

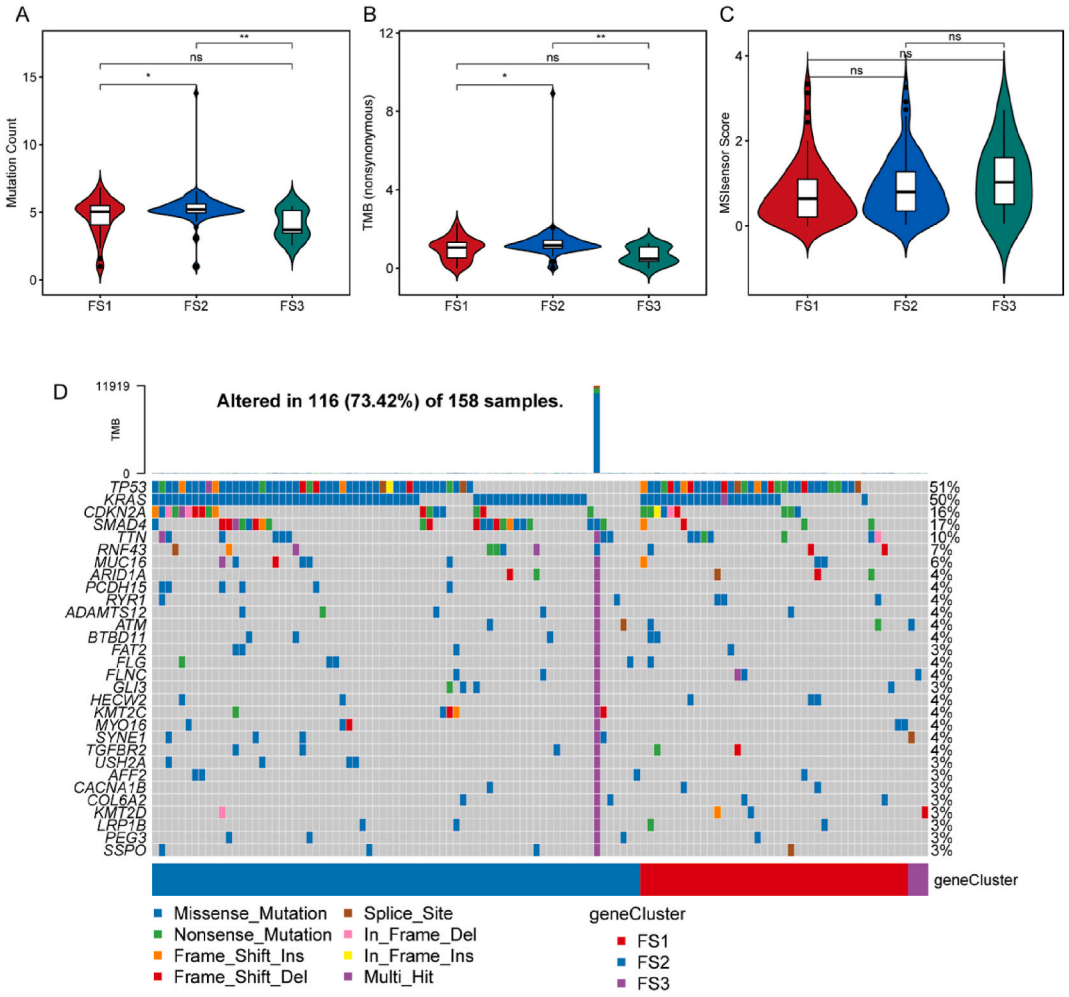

Fig. 4. Relationship between Ferroptosis subtypes and TMB and mutations. (A–C) Comparison of Mutation count (A), TMB (B), and MSI (C) among different Ferroptosis subtypes in PAAD. (D) PAAD waterfall plot showing the mutation feature genes of different Ferroptosis subtypes (FS1, FS2, and FS3). *p < 0.05, **p < 0.01, **p < 0.001.TMB: Tumor mutation burden.MSI: Microsatellite Instability.

subtypes were observed. Kaplan–Meier curves of 22 immune cells showed that activated, central memory $CD8^+$, and natural killer T cells were associated with poor prognosis, while eosinophils were associated with better prognosis (Supplementary Figs. 5A–D). We found that the FS1 and FS2 subtypes exhibited similar immune cell infiltration scores, which were higher than infiltration in the FS3 subtype. When comparing the four prognostic immune cells, significant statistical differences were observed for all four immune cells in the TCGA-PAAD cohort (Fig. 6C–F), and for activated T cells, central memory $CD8^+$ T cells, and eosinophils in the PACA-CA cohort (Fig. 6G–J); the trend of differences was consistent in both datasets. These results suggest that ferroptosis subtypes reflect the immune status of PAAD and could be used to identify suitable patients for mRNA vaccination.

2.6. Ferroptosis landscape of PAAD

We constructed a ferroptosis landscape of PAAD based on the expression profiles of FRGs in each patient (Fig. 7A). As shown in Fig. 7B, the horizontal axis (PCA1) is correlated with various immune cells, with the highest positive correlation observed for activated B cells, eosinophils, macrophages, mast cells, and follicular T cells, whereas the vertical axis (PCA2) is negatively correlated with most immune cell infiltrations. Within the same subtype, we also observed different intracluster heterogeneities. Based on the trajectory position of the sample groups, we further classified all samples into seven states (Fig. 7C). The endpoint states 1, 2, and 6, were selected for analysis. The proportions of these states in the different ferroptosis subtypes are shown in Fig. 7D. Prognostic analysis showed significant survival differences among the three states: state 6 had the best prognosis, while the curves of states 1 and 2 were concentrated (Fig. 7E). This was similar to the FS1, FS2, and FS3 categories. Significant differences were observed in the 28 immune cell scores among the different states (Fig. 7F). Overall, the ferroptosis landscape based on subtype could be used to identify the ferroptosis status of patients with PAAD and predict their prognosis, which is beneficial for personalized mRNA vaccine therapy

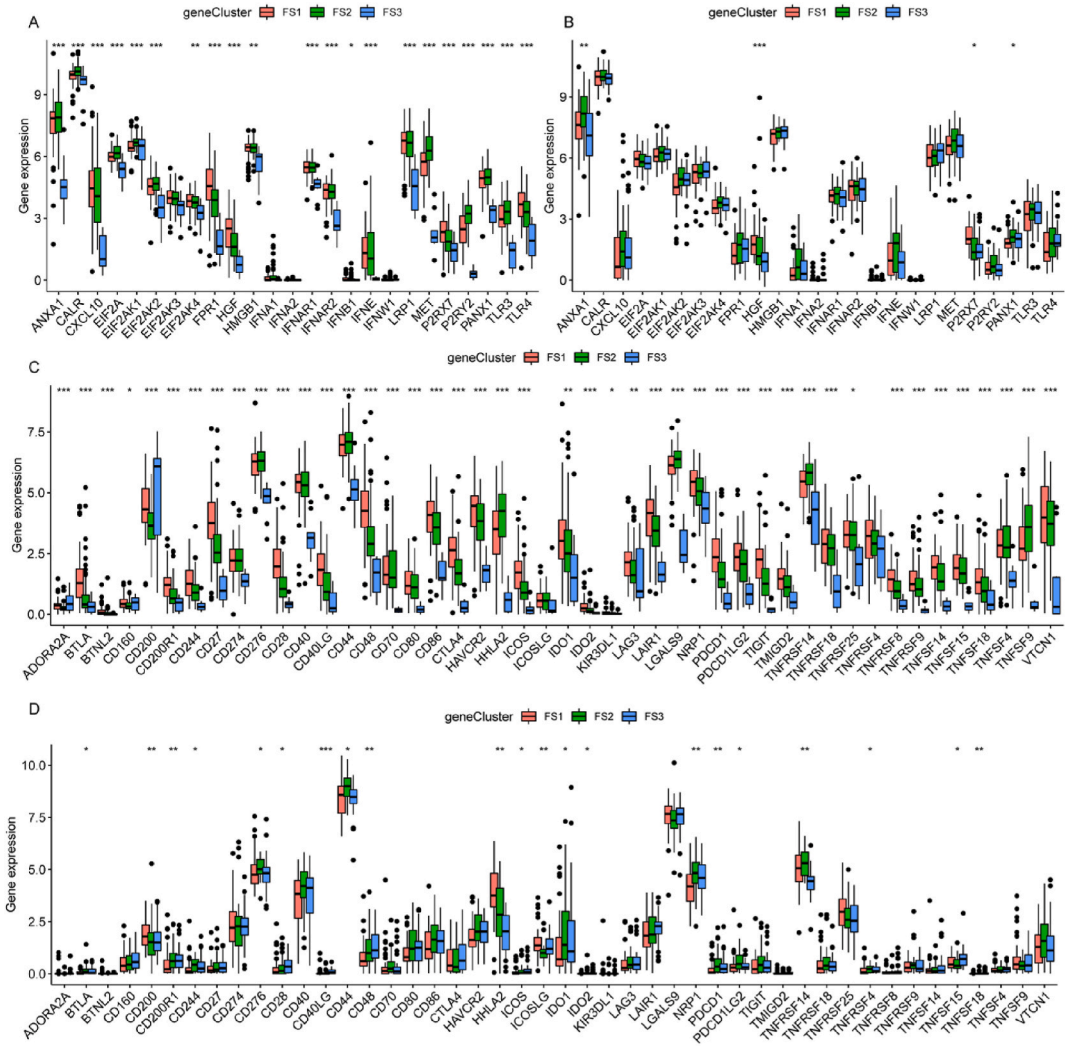

Fig. 5. The relationship between ferroptosis subtypes and ICD and ICP regulatory genes. (A–B) Differential expression of ICD regulatory genes in the three ferroptosis subtypes in the TCGA-PAAD (A) and PACA-CA (B) cohorts. C-D Differential expression of ICP genes in the three ferroptosis subtypes in the TCGA-PAAD (C) and PACA-CA (D) cohorts. *p < 0.05, **p < 0.01, ***p < 0.001, ****p < 0.0001.ICD: Immunogenic cell death. ICP: Immune checkpoint inhibitors.

selection.

2.7. *Identifying central ferroptosis genes and co-expressing FRG modules in PAAD*

The identification of key FRGs could help determine whether patients are suitable for mRNA vaccine administration. To identify key genes, we constructed a weighted gene co-expression network analysis (WGCNA) of FRGs. In the scale-free network, the soft-threshold power was set to six (Fig. 8A). The gene matrix was transformed into an adjacency matrix and a topological matrix adjacency matrix. Each gene module contained at least 20 genes. The characteristic genes of each module were calculated and similar modules were merged. Eleven modules were obtained, with the gray module representing unassigned genes (Fig. 8B–C). Significant differences were observed in the eigengene scores of the modules among different ferroptosis subtypes, with the green and magenta modules being higher in FS3 than in FS1 and FS2, whereas FS3 was lower than FS1 and FS2 in the remaining modules (Fig. 8D). After stepwise regression to eliminate collinear factors, multivariate COX analysis showed that only the green module was an independent prognostic factor (Fig. 8E), which contained 91 genes (Fig. 8F). Prognostic analysis based on the green module score showed that patients with a high score had a significantly better prognosis than those with a low score (Fig. 8G). In addition, genes in the green module were significantly enriched in immune-related functions and pathways such as cytokine-cytokine receptor interactions, hormone regulation, and the cAMP pathway (Fig. 8H–I). Genes in the green module included *MASP2, RLN1, GDF9, CRH, RXRA, ACVR1C, ACVR2B, FGF17, MSTN, GNAI1, MPL, MTNR1B, THRA, SFTPD,* and *CDNF.* Therefore, hub genes could serve as biomarkers

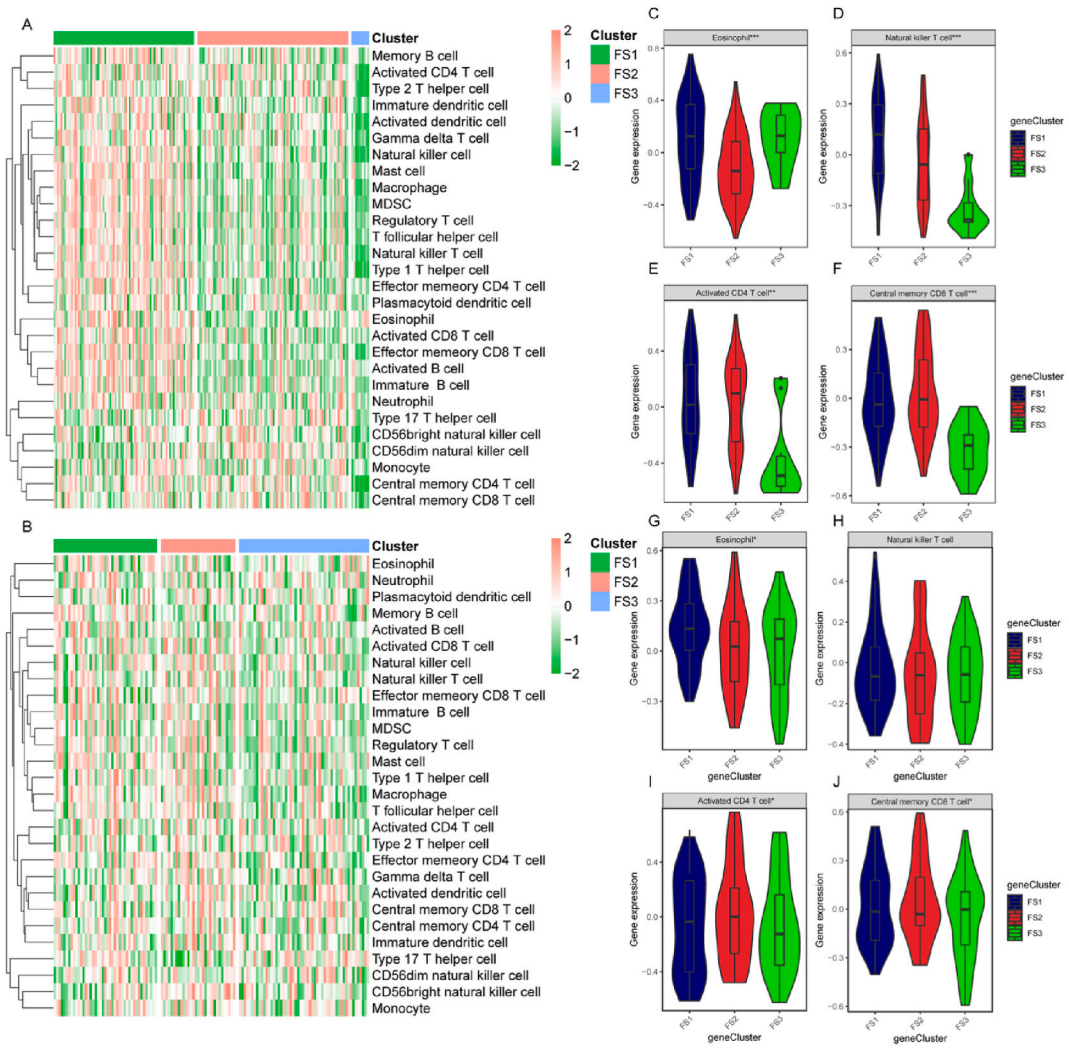

Fig. 6. Cellular and molecular characteristics of the ferroptosis subtype. (A–B) Heatmaps of the enrichment scores of 28 immune cell markers for the ferroptosis subtype in the TCGA-PAAD and PACA-CA cohorts, respectively. (C–F) Differential enrichment scores of activated T cells, central memory $CD8^+$ T cells, eosinophils, and natural killer T cells in the TCGA-PAAD cohort. (G–J) Differential enrichment scores of activated T cells, central memory $CD8^+$ T cells, eosinophils, and natural killer T cells in the PACA-CA cohort. *$p < 0.05$, **$p < 0.01$, ***$p < 0.001$.

for predicting the prognosis of patients with PAAD and might help to identify suitable patients for mRNA vaccines.

3. Discussion

Pancreatic cancer is an extremely malignant gastrointestinal tumor with a low surgical resection rate and insensitivity to traditional treatments, such as radiation and chemotherapy, resulting in a 5-year survival rate of only approximately 10%. Although studies have reported improved therapeutic efficacy for melanoma by combining tumor vaccines with ICPs or chemotherapy agents, current immunotherapy has not yielded improved results for pancreatic cancer. This may be related to the unique immune suppression state of the TME in pancreatic cancer. Therefore, reducing the immune evasion of pancreatic cancer cells and enhancing the body's immune response to pancreatic cancer is of great importance. In this study, we investigated the potential of ferroptosis-related tumor vaccines for pancreatic cancer treatment. Ferroptosis, a form of regulated cell death, was explored as a mechanism to induce an immune response against cancer cells. By triggering ferroptosis in cancer cells, these vaccines have the potential to expose cancer-specific antigens that can be recognized by the immune system. This recognition can stimulate the production of cancer-specific T cells and other immune cells, facilitating a targeted attack on cancer cells.

This is the first study to explore potential of FRGs as tumor antigens for mRNA vaccines in pancreatic cancer. Database analysis showed that in terms of mutated genomic fragments and number of mutations, *KRAS* and *TP53* were the most frequently mutated genes. In addition, *KRAS* mutations have been implicated in the pathogenesis of pancreatic cancer [28], potentially increasing ROS in

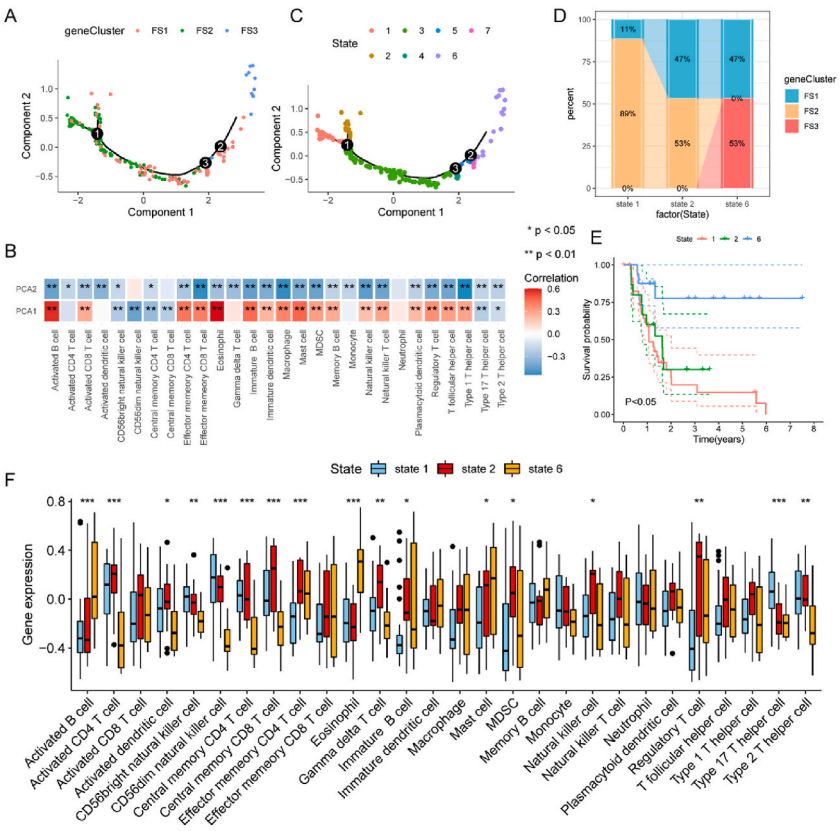

Fig. 7. Ferroptosis landscape of PAAD. (A) Ferroptosis landscape of PAAD constructed using the ferroptosis gene expression profiles of each patient. The position of each patient in the immune landscape is shown, with color corresponding to the identified ferroptosis subtypes, representing the overall characteristics of Ferroptosis related tumor microenvironment. (B) Correlation of PCA1/2 with immune modules. (C) PAAD patients reclassified based on their position into state 1, 2, 3, 4, 5, 6, and 7. (D) Proportions of ferroptosis subtypes in patients from different states. (E) Survival curves of patients from different states. It can be seen that there are differences in prognosis among patients from different states. (F) Comparison of the immune cell scores in the 28 immune cells in patients from different states. *p < 0.05, **p < 0.01, ***p < 0.001. (For interpretation of the references to color in this figure legend, the reader is referred to the Web version of this article.)

pancreatic cancer cells and inducing the synthesis of the antioxidant glutathione. Subsequently, we focused on identifying FRGs as potential mRNA antigens. *AGPS, KDM5A, NRAS,* and *OSBPL9* were identified as good candidates. These genes are highly expressed in tumor tissues and closely associated with TNM staging and OS/FPS prognosis. They can be directly processed and presented by APCs to T cells, recognized by B cells, activate tumor immune responses, and induce ferroptosis of tumor cells, further inhibiting tumor progression and improving the immunosuppressive state in pancreatic cancer TME.

Pancreatic cancer cells have significantly increased activity of system xc-to obtain more cysteine, the precursor of glutathione. However, normal cells require only low levels of cysteine for survival compared to cancer cells. Studies have shown that targeting system xc-to reduce cysteine uptake and subsequently lower glutathione synthesis leads to the accumulation of intracellular reactive oxygen species and induces ferroptosis in pancreatic cancer cells. This approach significantly prolonged the survival time of pancreatic tumor-bearing mice [29]. Therefore, selecting genes related to ferroptosis as mRNA vaccine targets for pancreatic cancer has significant implications for combination therapy of pancreatic cancer. AGPS is an enzyme that plays a critical role in the biosynthesis of ether lipids, which are important structural and signaling molecules in cells. Overexpression of AGPS has been shown to alter the balance of various lipids, including controlling fatty acid, eicosanoid, and acylglycerophospholipid metabolism to favor the generation of oncogenic signaling lipids, such as LPAe and lysophosphatidic acid (LPA), resulting in increased cancer cell proliferation and survival [30]. Another research found that AGPS plays a critical role in producing MUFA-linked ether phospholipids, which are essential for maintaining the redox balance in mitochondria of certain pancreatic cancer cells [31]. When AGPS is disrupted, these cells become more susceptible to cell death upon mitochondrial complex I inhibition, due to increased mitochondrial reactive oxygen species and lipid peroxidation. This highlights the importance of AGPS and its products in the survival mechanism of these cancer cells under stress conditions. Because of its key role in lipid metabolism and synthesis pathways, AGPS might be tightly linked to ferroptosis in tumor cells; however, there is no direct evidence to confirm the association. *KDM5A* (also known as *JARID1A or RBP2*) is overexpressed in various solid tumors and is closely associated with tumor growth, metastasis, drug resistance, and poor prognosis [32]. You et al. [33] found that inhibiting KDM5A could increase the expression of MPC1 and reduce the sensitivity of erlotinib-tolerant persistent head and neck cancer cells to ferroptosis induction, and demonstrated that its effect was related to the reduction of mesenchymal traits and

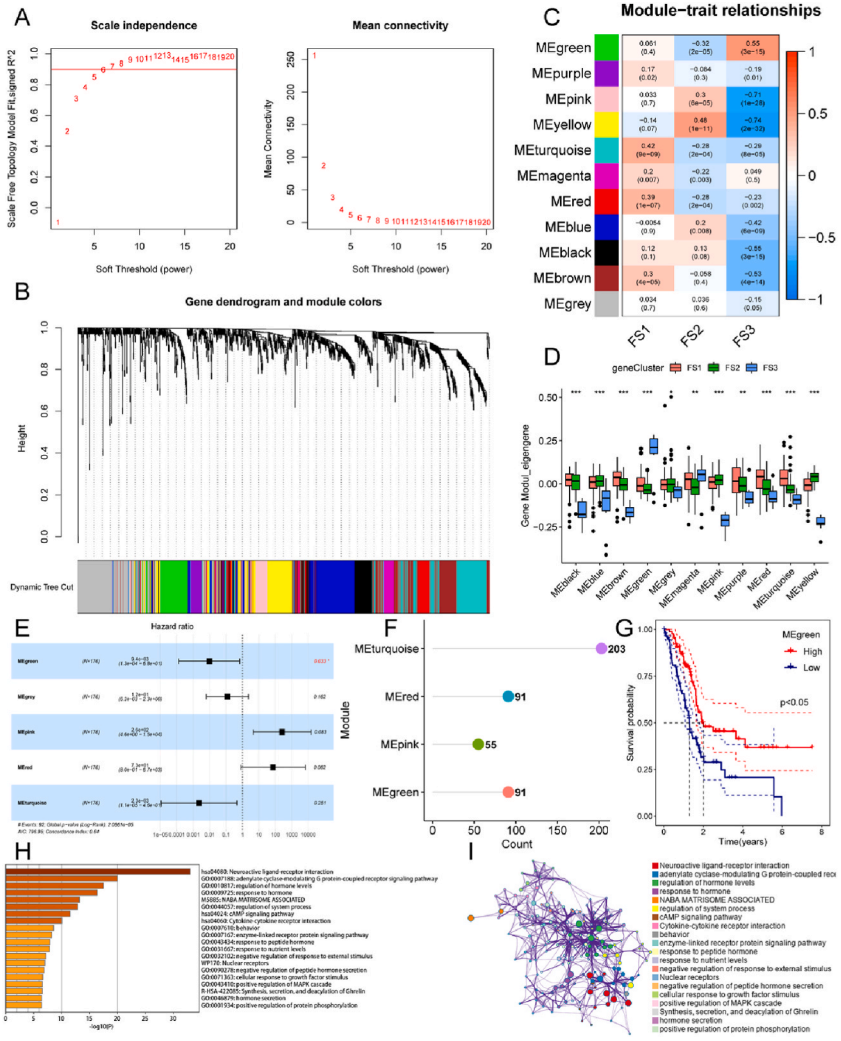

Fig. 8. Identification of core ferroptosis genes in PAAD. (A) Determination of the optimal soft threshold value for WGCNA. (B) WGCNA clustering tree. (C) The 11 modules obtained by WGCNA. (D) Comparison of ferroptosis subtypes' scores in different modules. (E) Multiple-factor Cox analysis of scores in different modules. (F) Number of genes in each module in the multiple-factor Cox analysis. (G) Prognostic curve for MEgreen, which shows a significant difference. (H–I) Functional enrichment of genes in the MEblue module.

glutaminolysis; therefore, KDM5A could be a good treatment option for drug-resistant tumor cells. Dan et al. [34] reveal that KDM5A, along with KDM5C, is found to be highly expressed in gemcitabine-resistant PDAC cells compared to sensitive cells, and manipulating its expression can affect the cells' drug resistance. Specifically, knocking down KDM5A/C leads to reduced drug resistance, fewer cell colonies, and decreased invasiveness, while overexpression has the opposite effect. The study suggests that KDM5A/C may act downstream of CD44, a stem cell marker, to influence chemoresistance. This connection between KDM5A/C and CD44 could be significant for developing new biomarkers or therapeutic targets for PDAC. Simultaneously, studies have found that increasing the expression of KDM5A in tumor tissues could significantly improve the efficacy of anti-PD-1 therapy in mouse models of melanoma and colon cancer, indicating its important role in tumor immunotherapy [35]. Notably, the four candidate genes we identified might be used as tumor vaccines to induce ferroptosis in cancer cells, thereby enhancing the anti-tumor immune response in the pancreatic cancer TME.

To improve patient selection for immune response to ferroptosis-related antigens, we analyzed the expression profile of FRGs in PAAD and identified three ferroptosis subtypes. The results showed that there was a clear distinction between the three ferroptosis subtypes, and pancreatic cancer patients with the FS3 subtype had a better prognosis than those with the FS1 and FS2 subtypes in TCGA and PACA cohorts. The three ferroptosis subtypes also showed different TNM stage distributions. In addition to predicting the prognosis of patients with pancreatic cancer, ferroptosis subtyping can also indicate the immune response generated by mRNA vaccine treatment. For example, ferroptosis subtypes can reflect the expression levels of ICD regulators and ICPs. One of the key features of cancer cells undergoing ICD is the spatiotemporally coordinated release of DAMPs, such as ATP and HMGB1. Research has shown that in the early stages of ferroptotic cell death, cancer cells can secrete bright DAMPs, and the injection of early stage ferroptotic cells can

lead to protective immunity in a mouse tumor prophylactic vaccination model if the adaptive immune system is intact. In the late stages of ferroptosis, cancer cells no longer exhibit immunogenicity, which may be related to their inability to secrete DAMPs [36]. In the FS3 subtype, the downregulation of *HMGB1* expression in TCGA-PAAD cohort suggests that inducing early-stage ferroptosis in tumor cells using ferroptosis-related antigens could potentially trigger a potent antitumor immune response in the FS3 subtype.

The immune response to mRNA vaccines depends on the immune status of the tumor. However, our results showed that tumor cell infiltration and patient prognosis may exhibit different trends. We found that patients with FS1-type tumors had more immune cell infiltration, followed by FS2 then FS3, but FS3 had a better prognosis than FS2 and FS1. Specifically, higher scores for activated, central memory $CD8^+$, and natural killer T cells were associated with worse prognosis, while higher scores for eosinophils were associated with better prognosis. This may be because pancreatic cancer cells suppress the antitumor immune response by activating immune suppression pathways or secreting immune inhibitory molecules. In addition to inducing tumor ferroptosis, T cells may also undergo ferroptosis, which may weaken their immune response. T cells that lack GPX4 quickly accumulate membrane lipid peroxides and undergo ferroptosis [37]. Research has shown that the expression of CD36 increases in $CD8^+$ tumor-infiltrating lymphocytes. The inherent CD36 in T cells promotes the uptake of oxidized lipids and induces lipid peroxidation, leading to the dysfunction of $CD8^+$ T cells. These findings reveal that $CD8^+$ T cell ferroptosis is a novel mode of tumor immune suppression and emphasize the therapeutic potential of blocking CD36 to enhance anti-tumor immunity [38,39]. Therefore, the impact of immune cell infiltration on patient prognosis might depend on tumor type, the TME, and immune responses. Among the three subtypes, FS3 is likely to be an immune "cold" type, with the lowest overall immune cell infiltration score. Conversely, FS2 and FS1 might be immune "hot" types, with higher immune cell infiltration than FS3. We also compared the TMB and somatic mutation rates of the three subtypes, as higher TMB and somatic mutation rates are associated with stronger antitumor immunity. The results showed that the TMB and total mutation number were lower in FS3 than in FS2 and FS1, further supporting the idea that FS3 is an immune "cold" type and FS2 and FS1 are immune "hot" types. Therefore, mRNA vaccines could be effective for patients with the FS3 subtype by inducing immune cell infiltration, increasing anti-tumor immunity, and improving the TME by inducing tumor cell ferroptosis, thereby reducing the probability of immune escape by tumor cells. Due to the high heterogeneity of pancreatic cancer, we constructed a ferroptosis landscape for PAAD based on the expression profiles of FRGs in each patient. This map enabled identification of the ferroptosis status of each PAAD patient and predict their prognosis, which is helpful for personalized mRNA vaccine therapy. Furthermore, we performed WGCNA of FRGs and identified 11 functional modules. Only the eigengene core of the green module was found to be an independent prognostic factor, and the high-scoring groups had significantly better prognosis than the low-scoring groups. Genes in the green module were significantly enriched in immune-related functions and pathways, such as cytokine-cytokine receptor interaction, hormone regulation, and the cAMP pathway. These genes, including MASP2, RLN1, GDF9, CRH, and RXRA, could serve as biomarkers for predicting the prognosis of patients with PAAD and identifying suitable candidates for mRNA vaccine therapy.

This study was based on bioinformatics analysis using data from public databases, but there may be some limitations, for example, there is an overlap between the FS1 cluster and the FS2 and FS3 clusters. This overlap may be attributed to the dataset itself, yet it is discernible that FS2 and FS3 can be distinctly differentiated from each other, indicating that ferroptosis subtyping in this disease may be meaningful. The overlap of FS1 with FS2 and FS3 could be due to a similarity in patient cohorts. We aim to continuously increase the sample size in future research to minimize the overlap in ferroptosis subtypes and to better elucidate the potential clinical implications of ferroptosis subtyping. In addition, the accuracy and reliability of the data were crucial to the results of the study. Our results rely on extensive calculations and analyses, and further validation is required in cell and animal models. There is still much to understand in ferroptosis-related tumor vaccines for pancreatic cancer, and it is important to note that this approach is still in the early stages of development. However, our study shows promising results, and this approach could potentially offer a new avenue for treating pancreatic cancer in the future.

4. Materials and methods

4.1. Data collection and preprocessing

The PAAD dataset was downloaded from the UCSC Xena database (version 2020), GDC TCGA Pancreatic Adenocarcinoma (v23.0) (n = 182), selecting the FPKM data type and extracting data from "Primary solid tumor" (01A). The data were then converted to the TPM format. The data conversion to TPM format involved normalization of the raw read counts to account for both the gene length and sequencing depth, enabling comparison across samples. The "Masked Somatic Mutation" data was selected as the somatic mutation data of PAAD patients, and VarScan software was used for data preprocessing. Somatic mutation visualization was achieved through the 'maftools' R package, which created illustrative plots representing the mutation landscape of the dataset. Clinical data, including age, TNM staging, and survival status, were also downloaded. Patients lacking comprehensive clinical information were excluded, resulting in a total of 176 patients with available survival information being retained for analysis. Gene expression data and survival information (including survival time and status) from the PACA-CA pancreatic cancer dataset were downloaded from the International Cancer Genome Consortium database. Patient samples without clinical staging and survival information were excluded, resulting in 122 tumor samples for this study. Additionally, 424 FRGs, including driver genes, inhibitor genes, and markers, were extracted from FerrDB (www.zhounan.org/ferrdb/) [15]. 25 immunogenic cell death genes (ICD) and 46 immune checkpoint (ICP) genes were obtained from previous literature [16,17].

4.2. Identification of tumor antigens

4.2.1. cBioPortal and GEPIA analyses

We integrated RNA-sequencing data from TCGA and other databases using the cBio Cancer Genomics Portal (v 4.1.3) (http://www.cbioportal.org) [18] to compare PAAD gene mutations. Microsatellite instability (MSI) and tumor mutation burden (TMB) data were also extracted from TCGA-PAAD patients. Differential gene expression was integrated using Gene Expression Profiling Interactive Analysis (GEPIA, v2.0; http://gepia2.cancer-pku.cn) [19]. Variance analysis was used to identify differentially expressed genes with $|\log2FC| > 1$ and a q-value <0.01. The Kaplan–Meier method was used to evaluate OS and progression-free survival (PFS) with a cutoff value of the median and compared them using a logarithmic rank test. Statistical significance was set at $p < 0.05$.

4.2.2. TIMER analysis

Tumor Immune Estimation Resource (TIMER, v2.0; https://cistrome.shinyapps.io/timer/) [20] was used to analyze the relationship between tumor-infiltrating immune cell abundance and potential tumor antigens based on gene expression, somatic mutation, clinical outcome, and somatic copy number alteration modules. For correlation analyses, TIMER employs Spearman's correlation, a non-parametric statistical method that measures the association between two variables, irrespective of whether they follow a normal distribution. In statistical analysis, a p-value <0.05 is typically considered to be significant. This criterion is also used in TIMER to determine the significance of results.

4.2.3. Developing and validating the ferroptosis subtypes

Ferroptosis subtypes were developed and validated by clustering FRGs using the "ConsensusClusterPlus" R package [21] based on expression profiles. A consensus matrix was constructed to identify the corresponding ferroptosis subtypes and gene modules. The median algorithm with the 1—Pearson correlation distance metric was used for partitioning and repeated 200 times with 80% of patients randomly sampled in each iteration. The clustering set range was 2–9, and the optimal partition was defined by evaluating the consensus matrix and cumulative distribution function. The ferroptosis subtypes were then validated in an independent PACA-CA cohort using the same settings.

4.2.4. Prognostic evaluation of ferroptosis subtypes

We used the log-rank test to evaluate the prognostic value of the ferroptosis subtypes. Variance analysis was used to determine the correlation between ferroptosis subtypes and ferroptosis-related molecular and cellular characteristics. The chi-square test was used to screen for the most commonly mutated genes. Single-sample Gene Set Enrichment Analysis (ssGSEA) from the GSVA package [22] was used to calculate the immune enrichment scores for each sample, which quantified the coordinated gene up- or downregulation within a sample.

4.2.5. Gene co-expression networks

The "WGCNA" R package [23] was used to screen modules of FRGs. The pickSoftThreshold function was used to calculate the soft threshold, with six being the optimal value. The soft threshold was then used to construct a scale-free network and topological matrix with hierarchical clustering to calculate eigengenes. Module-to-module correlations were constructed based on module eigengenes, and hierarchical clustering was performed. Functional enrichment analysis was performed using the Metascape database (www.metascape.org/) [24], which included the Kyoto Encyclopedia of Genes and Genomes(KEGG, v109.0) and Gene Ontology [25,26]. Statistical significance was set at Adj. $p < 0.05$.

4.2.6. Construction of ferroptosis landscape in TME

Utilizing graph-based dimensionality reduction analysis, Monocle package [27] with a Gaussian distribution was used to visualize the distribution of ferroptosis subtypes among patients. The maximum number of components was set to four and the discriminatory dimensionality reduction method "DDRtree" was employed. Finally, the functional map of ferroptosis subtypes was color-coded, and the cell trajectories were visualized to construct the ferroptosis landscape.

4.3. Statistical analysis

All statistical analyses were performed using R software (version 4.1.1). The Wilcoxon rank-sum test was used to compare differences between two groups, It is applicable to continuous variables and assists in determining whether two samples originate from the same population. And the Kruskal–Wallis test was used to evaluate differences among more than two groups, it amalgamate all observations from the samples and rank them, followed by assigning ranks to these values. This ranking takes into consideration the relative magnitude of the observations across all samples. Subsequently, a test statistic is derived from the differences in the sum of ranks for each sample, which is used to determine if the differences between the sample groups are statistically significant. Spearman's correlation analysis was used to assess the correlation between variables, it is a statistical method used to measure the non-linear relationship between two variables. It was introduced by psychologist Charles Spearman and is commonly used to assess rank-order correlations between different variables, especially when data do not meet normal distribution criteria or contain outliers. Statistical significance was set at $p < 0.05$.

5. Conclusions

We identified four FRGs (AGPS, KDM5A, NRAS, and OSBPL9) that could be used for mRNA vaccines. Based on the analysis of the FRG expression profile and WGCNA, we determined three minor ferroptosis subtypes, which were validated in different cohorts, with different clinical prognosis and tumor immune status. Of the subtypes, FS3 may be more suitable for mRNA therapy.

Funding

This research received no external funding

Data availability

Sharing research data helps other researchers evaluate your findings, build on your work and to increase trust in your article. We encourage all our authors to make as much of their data publicly available as reasonably possible. Please note that your response to the following questions regarding the public data availability and the reasons for potentially not making data available will be available alongside your article upon publication.

Additional information

No additional information is available for this paper.

CRediT authorship contribution statement

Ting Yan: Writing – original draft, Software, Methodology, Formal analysis, Data curation. **Lingxiang Wang:** Writing – review & editing, Supervision, Project administration, Conceptualization.

Declaration of competing interest

The authors declare that they have no known competing financial interests or personal relationships that could have appeared to influence the work reported in this paper.

Appendix A. Supplementary data

Supplementary data to this article can be found online at https://doi.org/10.1016/j.heliyon.2024.e27194.

References

[1] R.L. Siegel, K.D. Miller, H.E. Fuchs, A. Jemal, Cancer statistics, 2022, CA, Cancer J. Clin. 72 (2022) 7–33, https://doi.org/10.3322/caac.21708.
[2] L. Rahib, B.D. Smith, R. Aizenberg, A.B. Rosenzweig, J.M. Fleshman, L.M. Matrisian, Projecting cancer Incidence and deaths to 2030: the unexpected burden of thyroid, liver, and pancreas cancers in the United States, Cancer Res. 74 (2014) 2913–2921, https://doi.org/10.1158/0008-5472.CAN-14-0155.
[3] N. Zhou, J. Bao, J. Huang, V. Lok, C.H. Ngai, L. Zhang, J. Yuan, X.Q. Lao, K. Ng, C. Chong, Z.-J. Zheng, M.C.S. Wong, Worldwide burden of, risk factors for, and trends in pancreatic cancer, Gastroenterology 160 (2021) 744–754, https://doi.org/10.1053/j.gastro.2020.10.007.
[4] K. Spanknebel, K.C. Conlon, Advances in the surgical management of pancreatic cancer, Cancer J. Sudbury Mass 7 (2001) 312–323.
[5] H.A. Burris, M.J. Moore, J. Andersen, M.R. Green, M.L. Rothenberg, M.R. Modiano, M.C. Cripps, R.K. Portenoy, A.M. Storniolo, P. Tarassoff, R. Nelson, F. A. Dorr, C.D. Stephens, D.D. Von Hoff, Improvements in survival and clinical benefit with gemcitabine as first-line therapy for patients with advanced pancreas cancer: a randomized trial, J. Clin. Oncol. 15 (1997) 2403–2413, https://doi.org/10.1200/JCO.1997.15.6.2403.
[6] M.S. Carlino, J. Larkin, G.V. Long, Immune checkpoint inhibitors in melanoma, Lancet 398 (2021) 1002–1014, https://doi.org/10.1016/S0140-6736(21)01206-X.
[7] Y. Yuan, F. Gao, Y. Chang, Q. Zhao, X. He, Advances of mRNA vaccine in tumor: a maze of opportunities and challenges, Biomark. Res. 11 (2023) 6, https://doi.org/10.1186/s40364-023-00449-w.
[8] N. Pardi, M.J. Hogan, F.W. Porter, D. Weissman, mRNA vaccines — a new era in vaccinology, Nat. Rev. Drug Discov. 17 (2018) 261–279, https://doi.org/10.1038/nrd.2017.243.
[9] A.Z. Tóth, A. Szabó, E. Hegyi, P. Hegyi, M. Sahin-Tóth, D. Bittencourt, D.-Y. Wu, K.W. Jeong, D.S. Gerke, L. Herviou, I. Ianculescu, R. Chodankar, K.D. Siegmund, M.R. Stallcup, Z. Tong, Y. Fan, W. Zhang, J. Xu, J. Cheng, M. Ding, H. Deng, Z. Jancsó, M. Sahin-Tóth, C. Feig, A. Gopinathan, A. Neesse, D.S. Chan, N. Cook, D. A. Tuveson, The pancreas cancer microenvironment, Clin. Cancer Res. 18 (2012) 4266–4276, https://doi.org/10.1158/1078-0432.CCR-11-3114.
[10] A. Párniczky, B. Kui, A. Szentesi, A. Balázs, Á. Szűcs, D. Mosztbacher, J. Czimmer, P. Sarlós, J. Bajor, S. Gódi, Á. Vincze, A. Illés, I. Szabó, G. Pár, T. Takács, L. Czakó, Z. Szepes, Z. Rakonczay, F. Izbéki, J. Gervain, A. Halász, J. Novák, S. Crai, I. Hritz, C. Góg, J. Sümegi, P. Golovics, M. Varga, B. Bod, J. Hamvas, M. Varga-Müller, Z. Papp, M. Sahin-Tóth, P. Hegyi, Enzymatic targeting of the stroma ablates physical barriers to treatment of pancreatic ductal adenocarcinoma, Cancer Cell 21 (2012) 418–429, https://doi.org/10.1016/j.ccr.2012.01.007.
[11] I. Haque, A. Subramanian, S. Banerjee, S.K. Banerjee, Current and emerging perspectives on immunotherapy for pancreatic cancer, Transl, Cancer Res. 6 (2017) S331, https://doi.org/10.21037/tcr.2017.03.48. –S336.
[12] B.R. Stockwell, Ferroptosis turns 10: emerging mechanisms, physiological functions, and therapeutic applications, Cell 185 (2022) 2401–2421, https://doi.org/10.1016/j.cell.2022.06.003.
[13] L. Zhao, X. Zhou, F. Xie, L. Zhang, H. Yan, J. Huang, C. Zhang, F. Zhou, J. Chen, L. Zhang, Ferroptosis in cancer and cancer immunotherapy, Cancer Commun. 42 (2022) 88–116, https://doi.org/10.1002/cac2.12250.

[14] Z. Chen, J. Lin, S. Feng, X. Chen, H. Huang, C. Wang, Y. Yu, Y. He, S. Han, L. Zheng, G. Huang, H. Wang, P. An, E. Xie, Q. Wu, X. Fang, H. Gao, Z. Zhang, Y. Li, X. Wang, J. Zhang, G. Li, L. Yang, W. Liu, J. Min, F. Wang, Characterization of ferroptosis in murine models of hemochromatosis, Hepatology 66 (2017) 449–465, https://doi.org/10.1002/hep.29117.
[15] M. Mehravar, A. Shirazi, M. Nazari, M. Banan, N. Zhou, J. Bao, FerrDb: a manually curated resource for regulators and markers of ferroptosis and ferroptosis-disease associations, Database (2020) 2020, https://doi.org/10.1093/database/baaa021, baaa021.
[16] X. Huang, T. Tang, G. Zhang, T. Liang, Identification of tumor antigens and immune subtypes of cholangiocarcinoma for mRNA vaccine development, Mol. Cancer 20 (2021) 50, https://doi.org/10.1186/s12943-021-01342-6.
[17] X. Huang, G. Zhang, T. Tang, T. Liang, Identification of tumor antigens and immune subtypes of pancreatic adenocarcinoma for mRNA vaccine development, Mol. Cancer 20 (2021) 44, https://doi.org/10.1186/s12943-021-01310-0.
[18] J. Gao, B.A. Aksoy, U. Dogrusoz, G. Dresdner, B. Gross, S.O. Sumer, Y. Sun, A. Jacobsen, R. Sinha, E. Larsson, E. Cerami, C. Sander, N. Schultz, Integrative analysis of complex cancer genomics and clinical profiles using the cBioPortal, Sci. Signal. 6 (2013), https://doi.org/10.1126/scisignal.2004088.
[19] Z. Tang, C. Li, B. Kang, G. Gao, C. Li, Z. Zhang, GEPIA: a web server for cancer and normal gene expression profiling and interactive analyses, Nucleic Acids Res. 45 (2017) W98, https://doi.org/10.1093/nar/gkx247. –W102.
[20] T. Li, J. Fan, B. Wang, N. Traugh, Q. Chen, J.S. Liu, B. Li, X.S. Liu, TIMER: a web server for comprehensive analysis of tumor-infiltrating immune cells, Cancer Res. 77 (2017), https://doi.org/10.1158/0008-5472.CAN-17-0307 e108–e110.
[21] M.Y. Suh, T.W. Kim, H. Lee, J. Shin, J. Kim, H. Jang, H.J. Kim, S. Kim, E. Cho, H. Youn, M.D. Wilkerson, D.N. Hayes, ConsensusClusterPlus: a class discovery tool with confidence assessments and item tracking, Bioinformatics 26 (2010) 1572–1573, https://doi.org/10.1093/bioinformatics/btq170.
[22] S. Hänzelmann, R. Castelo, J. Guinney, GSVA: gene set variation analysis for microarray and RNA-Seq data, BMC Bioinf. 14 (2013) 7, https://doi.org/10.1186/1471-2105-14-7.
[23] P. Langfelder, S. Horvath, WGCNA: an R package for weighted correlation network analysis, BMC Bioinf. 9 (2008) 559, https://doi.org/10.1186/1471-2105-9-559.
[24] Y. Zhou, B. Zhou, L. Pache, M. Chang, A.H. Khodabakhshi, O. Tanaseichuk, C. Benner, S.K. Chanda, Metascape provides a biologist-oriented resource for the analysis of systems-level datasets, Nat. Commun. 10 (2019) 1523, https://doi.org/10.1038/s41467-019-09234-6.
[25] The Gene Ontology Consortium, Gene Ontology Consortium: going forward, Nucleic Acids Res. 43 (2015) D1049–D1056, https://doi.org/10.1093/nar/gku1179.
[26] M. Kanehisa, KEGG: Kyoto Encyclopedia of genes and genomes, Nucleic Acids Res. 28 (2000) 27–30, https://doi.org/10.1093/nar/28.1.27.
[27] P. Perešíni, M. Kuźniar, D. Kostić, Monocle, in: Proc. 11th ACM Conf. Emerg. Netw. Exp. Technol. (2015) 1–13, https://doi.org/10.1145/2716281.2836117.
[28] W. Qin, P.M. Kutny, R.S. Maser, S.L. Dion, J.D. Lamont, Y. Zhang, G.A. Perry, H. Wang, N. Waddell, K. Quek, M.C.J. Quinn, A.J. Robertson, M.Z.H. Fadlullah, T. J.C. Bruxner, A.N. Christ, I. Harliwong, S. Idrisoglu, S. Manning, C. Nourse, E. Nourbakhsh, S. Wani, P.J. Wilson, E. Markham, N. Cloonan, M.J. Anderson, J. L. Fink, O. Holmes, S.H. Kazakoff, C. Leonard, F. Newell, B. Poudel, S. Song, D. Taylor, N. Waddell, S. Wood, Q. Xu, J. Wu, M. Pinese, M.J. Cowley, H.C. Lee, M. D. Jones, A.M. Nagrial, J. Humphris, L.A. Chantrill, V. Chin, A.M. Steinmann, A. Mawson, E.S. Humphrey, E.K. Colvin, A. Chou, C.J. Scarlett, A.V. Pinho, M. Giry-Laterriere, I. Rooman, J.S. Samra, J.G. Kench, J.A. Pettitt, N.D. Merrett, C. Toon, K. Epari, N.Q. Nguyen, A. Barbour, N. Zeps, N.B. Jamieson, J. S. Graham, S.P. Niclou, R. Bjerkvig, R. Grützmann, D. Aust, R.H. Hruban, A. Maitra, C.A. Iacobuzio-Donahue, C.L. Wolfgang, R.A. Morgan, R.T. Lawlor, V. Corbo, C. Bassi, M. Falconi, G. Zamboni, G. Tortora, M.A. Tempero, Australian Pancreatic Cancer Genome Initiative, A.J. Gill, J.R. Eshleman, C. Pilarsky, A. Scarpa, E.A. Musgrove, J.V. Pearson, A.V. Biankin, S.M. Grimmond, Whole genomes redefine the mutational landscape of pancreatic cancer, Nature 518 (2015) 495–501, https://doi.org/10.1038/nature14169.
[29] M.A. Badgley, D.M. Kremer, H.C. Maurer, K.E. DelGiorno, H.-J. Lee, V. Purohit, I.R. Sagalovskiy, A. Ma, J. Kapilian, C.E.M. Firl, A.R. Decker, S.A. Sastra, C. F. Palermo, L.R. Andrade, P. Sajjakulnukit, L. Zhang, Z.P. Tolstyka, T. Hirschhorn, C. Lamb, T. Liu, W. Gu, E.S. Seeley, E. Stone, G. Georgiou, U. Manor, A. Iuga, G.M. Wahl, B.R. Stockwell, C.A. Lyssiotis, K.P. Olive, Cysteine depletion induces pancreatic tumor ferroptosis in mice, Science 368 (2020) 85–89, https://doi.org/10.1126/science.aaw9872.
[30] D.I. Benjamin, A. Cozzo, X. Ji, L.S. Roberts, S.M. Louie, M.M. Mulvihill, K. Luo, D.K. Nomura, Ether lipid generating enzyme AGPS alters the balance of structural and signaling lipids to fuel cancer pathogenicity, Proc. Natl. Acad. Sci. USA 110 (2013) 14912–14917, https://doi.org/10.1073/pnas.1310894110.
[31] Z. Chen, I.-L. Ho, M. Soeung, E.-Y. Yen, J. Liu, L. Yan, J.L. Rose, S. Srinivasan, S. Jiang, Q. Edward Chang, N. Feng, J.P. Gay, Q. Wang, J. Wang, P.L. Lorenzi, L. J. Veillon, B. Wei, J.N. Weinstein, A.K. Deem, S. Gao, G. Genovese, A. Viale, W. Yao, C.A. Lyssiotis, J.R. Marszalek, G.F. Draetta, H. Ying, Ether phospholipids are required for mitochondrial reactive oxygen species homeostasis, Nat. Commun. 14 (2023) 2194, https://doi.org/10.1038/s41467-023-37924-9.
[32] P. Liu, H. Tang, B. Chen, Z. He, M. Deng, M. Wu, X. Liu, L. Yang, F. Ye, X. Xie, G.-J. Yang, M.-H. Zhu, X.-J. Lu, Y.-J. Liu, J.-F. Lu, C.-H. Leung, D.-L. Ma, J. Chen, The emerging role of KDM5A in human cancer, J. Hematol. Oncol.J Hematol Oncol 14 (2021) 30, https://doi.org/10.1186/s13045-021-01041-1.
[33] J.H. You, J. Lee, J.-L. Roh, Mitochondrial pyruvate carrier 1 regulates ferroptosis in drug-tolerant persister head and neck cancer cells via epithelial-mesenchymal transition, Cancer Lett. 507 (2021) 40–54, https://doi.org/10.1016/j.canlet.2021.03.013.
[34] D. Wang, Y. Zhang, Z. Liao, H. Ge, C. Güngör, Y. Li, KDM5 family of demethylases promotes CD44-mediated chemoresistance in pancreatic adenocarcinomas, Sci. Rep. 13 (2023) 18250, https://doi.org/10.1038/s41598-023-44536-2.
[35] Y. Shi, J. Sawada, G. Sui, E.B. Affar, J.R. Whetstine, F. Lan, H. Ogawa, M. Po-Shan Luke, Y. Nakatani, Y. Shi, L. Wang, Y. Gao, G. Zhang, D. Li, Z. Wang, J. Zhang, L.C. Hermida, L. He, Z. Wang, J. Si, S. Geng, R. Ai, F. Ning, C. Cheng, H. Deng, D.S. Dimitrov, Y. Sun, Y. Huang, D. Wang, X. Hu, Z. Wei, W. Wang, X. Liao, Enhancing KDM5A and TLR activity improves the response to immune checkpoint blockade, Sci. Transl. Med. 12 (2020), https://doi.org/10.1126/scitranslmed.aax2282 eaax2282.
[36] I. Efimova, E. Catanzaro, L. Van der Meeren, V.D. Turubanova, H. Hammad, T.A. Mishchenko, M.V. Vedunova, C. Fimognari, C. Bachert, F. Coppieters, S. Lefever, A.G. Skirtach, O. Krysko, D.V. Krysko, Vaccination with early ferroptotic cancer cells induces efficient antitumor immunity, J. Immunother. Cancer 8 (2020) e001369, https://doi.org/10.1136/jitc-2020-001369.
[37] M. Matsushita, S. Freigang, C. Schneider, M. Conrad, G.W. Bornkamm, M. Kopf, T cell lipid peroxidation induces ferroptosis and prevents immunity to infection, J. Exp. Med. 212 (2015) 555–568, https://doi.org/10.1084/jem.20140857.
[38] X. Ma, L. Xiao, L. Liu, L. Ye, P. Su, E. Bi, Q. Wang, M. Yang, J. Qian, Q. Yi, CD36-mediated ferroptosis dampens intratumoral CD8+ T cell effector function and impairs their antitumor ability, Cell Metabol. 33 (2021) 1001–1012.e5, https://doi.org/10.1016/j.cmet.2021.02.015.
[39] S. Xu, O. Chaudhary, P. Rodríguez-Morales, X. Sun, D. Chen, R. Zappasodi, Z. Xu, A.F.M. Pinto, A. Williams, I. Schulze, Y. Farsakoglu, S.K. Varanasi, J.S. Low, W. Tang, H. Wang, B. McDonald, V. Tripple, M. Downes, R.M. Evans, N.A. Abumrad, T. Merghoub, J.D. Wolchok, M.N. Shokhirev, P.-C. Ho, J.L. Witztum, B. Emu, G. Cui, S.M. Kaech, Uptake of oxidized lipids by the scavenger receptor CD36 promotes lipid peroxidation and dysfunction in CD8+ T cells in tumors, Immunity 54 (2021) 1561–1577.e7, https://doi.org/10.1016/j.immuni.2021.05.003.